ELSEVIER

Ceramics International 31 (2005) 803–809

CERAMICS INTERNATIONAL

www.elsevier.com/locate/ceramint

Soaking method for fabrication of alumina-based nanocomposites

Uraiwan Leela-adisorn, Takuya Matsunaga, Yoshitomo Kobayashi, Seong-Min Choi, Hideo Awaji*

Department of Materials Science and Technology, Nagoya Institute of Technology, Gokiso-cho, Showa-ku, Nagoya 466–8555, Japan

Received 28 June 2004; received in revised form 2 August 2004; accepted 12 September 2004
Available online 9 December 2004

Abstract

Previously published research proposed strengthening and toughening mechanisms of nanocomposites based on dislocation activities even in brittle ceramics. We reported that an intra-type nano-structure could only have the potential to improve strength and fracture toughness due to dislocations formed around the dispersed particles. In this research, nickel dispersed alumina nanocompsoites were fabricated using a novel soaking method, based on the developed strengthening and toughening mechanisms. Commercially available γ-alumina powder with high porosity was used as the starting materials. Secondary, particles were introduced into the nano-pores of the porous γ-alumina powder using a soaking method, where the alumina powder was soaked in a nickel nitrate solution under vacuum. During pre-calcination, nickel oxide particles were generated inside the nano-pores. The alumina powders were then reduced under hydrogen atmosphere to obtain nano-sized metallic nickel inside the γ-alumina grains. The alumina–nickel composite powders were sintered by pulse electric current sintering (PECS) technique with α-alumina seeds. The mechanical properties of specimens were investigated, such as density, three-point strength, and fracture toughness. The maximum strength of the alumina–nickel nanocomposites was 984 MPa after being sintered at 1450 °C with α-alumina seeds, where the specimen size was 2 mm × 2 mm × 10 mm. The maximum fracture toughness was 5.5 MPa $m^{1/2}$ after being sintered at 1350 °C with seeds measured by the single edge V-notched beam method.

Keywords: B. Nanocomposites; C. Strength; D. Al_2O_3; Fracture toughness; Soaking method

1. Introduction

Structural ceramics have low fracture toughness because of their ionic and covalent bonds, severely limiting the plastic deformation of ceramics due to dislocation activities. It is, therefore, hypothesized that a frontal process zone (FPZ) ahead of a crack tip is composed of nano-cracks rather than dislocations as is the case with metals. To overcome the inherent brittleness of ceramics, a new material design concept must be developed. The microstructure of nano-composites developed by Niihara [1] is constructed by dispersing second-phase nano-size particles within the matrix grains (intra-type nanostructure) and on the grain boundaries (inter-type nanostructure). The intra-type nano-structure produces thermal expansion mismatch between the matrix and second-phase particles and provides a marked improvement in several mechanical properties such as fracture strength, fracture toughness, creep resistance, thermal shock resistance, and wear resistance.

Ceramics-based nanocomposites have been fabricated using high speed sintering techniques, such as hot pressing and pulse electric current sintering (PECS) [2,3] because of their low sinterability. Intra-type nano-structure is particularly difficult to fabricate using a pressure-less sintering technique. In this paper, first, we summarize the toughening and strengthening mechanisms of nanocomposites introduced in our previous papers [4,5], and second, a newly developed soaking method for constructing an intra-type nano-structure will be proposed for alumina-based nanocomposites. Finally, experimental results for alumina–nickel nanocomposites will be shown and discussed.

* Corresponding author. Tel.: +81 52 735 5276; fax: +81 52 735 5276.
E-mail address: awaji@nitech.ac.jp (H. Awaji).

0272-8842/$30.00
doi:10.1016/j.ceramint.2004.09.007

2. Toughening and strengthening mechanisms

2.1. Dislocation activities

Intra-type nanocomposites consist of nano-particles dispersed within matrix grains. The characteristics of the intra-type nanocomposites result in the generation of thermally induced residual stresses after sintering. To clarify the role of the residual stresses around the dispersed particles in nanocomposites, Awaji and coworkers [4,6] analyzed residual stresses using a simplified model that consisted of a spherical particle within a concentric matrix sphere with axial symmetry, shown in Fig. 1, where we restrict our attention to the alumina-based nanocomposites to simplify the following discussion. Residual stresses numerically calculated on the particle-matrix boundary for alumina–nickel nanocomposites are shown in Table 1, where we assumed that the temperature difference between the sintered temperature and room temperature was 1570 °C and that the ratio of the particle/matrix radii was 1/5. In the table, symbols with suffix p indicate the properties of the particle (nickel) and symbols with suffix m are the properties of the matrix (alumina). It is noted that there is a large maximum shear stress on the particle/matrix boundary.

Lagerlöf et al. [7] reported that the temperature dependence of both basal and prism plane slips in an α-alumina single crystal could be described by a simple logarithmic law over a wide range of temperature:

$$\ln \tau_{cb} = \ln \tau_0 - 0.0052T, \quad (1)$$

and

$$\ln \tau_{cp} = \ln \tau_0 - 0.0026T, \quad (2)$$

where τ_{cb} and τ_{cp} represent the critical resolved shear stresses (CRSS) for basal and prism plane slips, respectively, T is temperature (K), and τ_0 is 109 and 9 GPa for basal and prism plane slips, respectively. Fig. 2 shows the temperature dependence of the CRSS for basal and prism plane slips in an α-alumina single crystal and the residual shear stress τ_{res} on the alumina–nickel boundary in the nanocomposites. It is noted that dislocation activities are possible in the alumina grains at temperatures ranging from about 800 to 1400 °C.

Table 1
The maximum shear stress along the particle-matrix boundary in alumina–nickel nanocomposites

System	Al_2O_3/Ni
$\alpha_m/\alpha_p \times 10^{-6}$ (K^{-1})	8.8/13.7
E_m/E_p (GPa)	380/207
ν_m/ν_p	0.21/0.31
τ_{max} (GPa)	1.06

At room temperature under the assumption of ΔT = 1570 °C and the ratio of the spherical particle and matrix radii is 1/5.

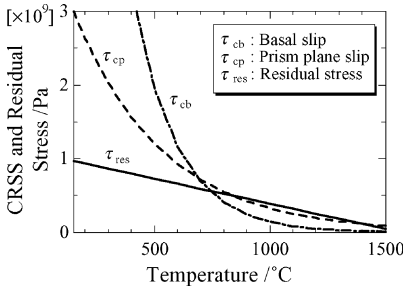

Fig. 2. Critical resolved shear stresses for α-alumina single crystal and residual stresses in alumina–nickel nanocomposites.

Mismatches in thermal expansion and Young's modulus between the matrix and the dispersed particles will yield highly localized residual stresses. These stresses are reduced quickly as distance from the boundary increases because of the nano-sized particles, which can generate only small defects such as dislocations in close proximity to the particles, as shown in Fig. 3A. Large-scale cracks or other large defects will be difficult to create in the nanocomposite system and only dislocations can disperse in matrix grains at high temperatures. These dislocations are believed to become nano-crack nuclei at room temperature because the CRSS at room temperature for prism plane slip is estimated to be 4.1 GPa from Eq. (2), which is higher than the theoretical strength of the α-alumina of 2.6 GPa. This fact suggests that further annealing is important in

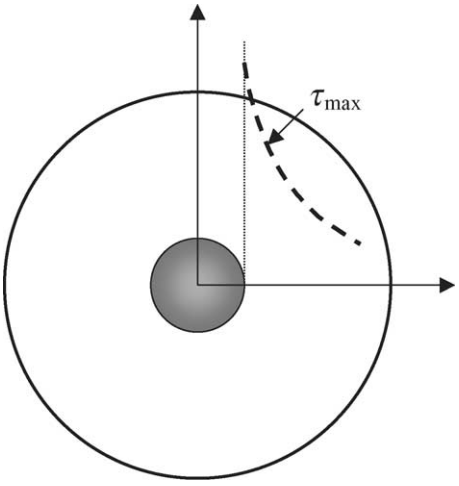

Fig. 1. A model of intra-type nano-structure.

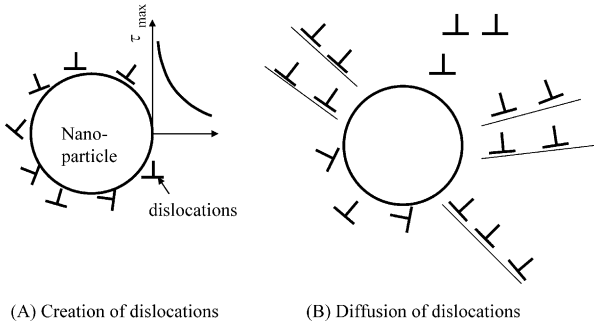

Fig. 3. Dislocation activities after sintering (A) and after annealing (B).

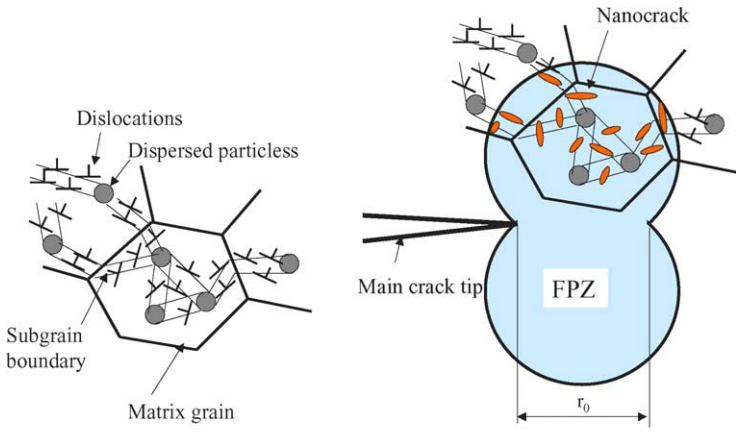

Fig. 4. Schematic description of the toughening mechanism in nanocomposites.

dispersing dislocations into the matrix grains, as shown in Fig. 3B.

2.2. Toughening mechanism

Fig. 4 shows a schematic illustration of the toughening mechanism of nanocomposites. Dispersed dislocations within the matrix grains after annealing for alumina–nickel nanocomposites are described in this figure. Sub-grain boundaries are generated around the nano-size nickel particles and these dislocations become sessile dislocations, shown in Fig. 4A. In this situation, when a tip of a propagating large crack reaches this area, these sessile dislocations in the matrix grains will operate as nano-crack nuclei in the vicinity of the propagating crack tip, shown in Fig. 4B. The high stress-state in the FPZ is then released by nano-crack nucleation, and the nano-cracks expand the FPZ size and consequently enhance the fracture toughness of the materials.

2.3. Strengthening mechanism

Sintered alumina has tensile residual stresses in the grains and grain boundaries because of anisotropic thermal expansion, Young's modulus along the crystalline axes, and the crystallographic mis-orientation across the grain boundaries. In the sintered polycrystalline alumina, therefore, it is conceivable that the large crack along a grain boundary created by synergetic effects of both residual stresses and processing defects will be equivalent to the grain size of the material and that the weakest crack generated along the boundary in the specimen dominates the strength of the specimen. The fracture toughness of grain boundaries is usually lower than that of the matrix grains. Hence, polycrystalline alumina ceramics exhibit mainly intergranular fracture mode, as schematically shown in Fig. 5A. Fig. 6A also shows the scanning electron microscopy (SEM) observation of the fracture surface of monolithic alumina.

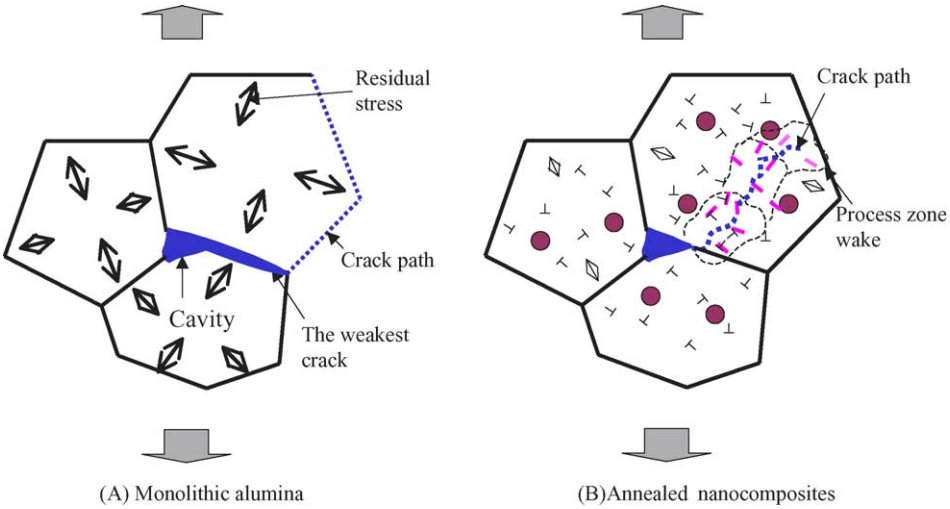

Fig. 5. Schematic explanation of the strengthening mechanism in nanocomposites.

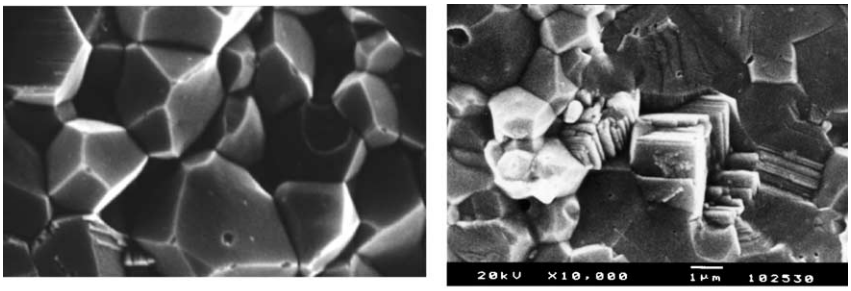

(A)Monolithicalumina (B) Alumina/5 vol%Cu nanocomposites

Fig. 6. SEM micrographs of fracture surfaces of monolithic alumina (A) and alumina–copper nanocomposites (B).

Nanocomposites, however, will yield dislocations around the particles, and the dislocation creation releases residual stresses in the matrix grains. Consequently, the defect size along the grain boundaries is reduced in nanocomposites, as shown in Fig. 5B. Also, the dislocations are difficult to move in ceramics at room temperature, serve as origins of small stress concentrations, and create nano-cracks around the propagating crack tip. These nano-cracks slightly reduce the strength of the alumina matrix and the reduction of both the residual stress along the grain boundaries and the strength in the matrix is attributable to a change in the fracture mode from that of intergranular fracture in monolithic alumina to that of transgranular fracture in nanocomposites. Also, the fracture surface of the transgranular mode of nanocomposites is not a simple planar cleavage plane. Several steps are frequently observed on the surface and this phenomenon is likely to be evidence of nano-cracking in the wake of the FPZ. Fig. 6B shows the SEM micrograph of the fracture surface of alumina–copper nanocomposites fabricated by us [5]. Reduction of both the defect size along the grain boundaries and the tensile residual stresses in the matrix grains by dislocation activities result in improvement of the strength of nanocomposites.

3. Experimental procedure

3.1. Soaking method

Based on the toughening and strengthening mechanisms of nanocomposites mentioned above, we propose a soaking method for constructing intra-type nano-structures. In this research, we use γ-alumina as a matrix. Commercially available γ-alumina powder consists of column-like primary particles and has an agglomerated form with many pores. The soaking technique is schematically shown in Fig. 7. First, the γ-alumina powder is soaked in nickel nitrate solution under vacuum. The γ-alumina–nickel solution composite powder is filtered and dried, following calcinations to get nickel oxide particles in the pores of the γ-alumina powder. The calcinated specimens were reduced under hydrogen atmosphere to obtain metallic nickel in the

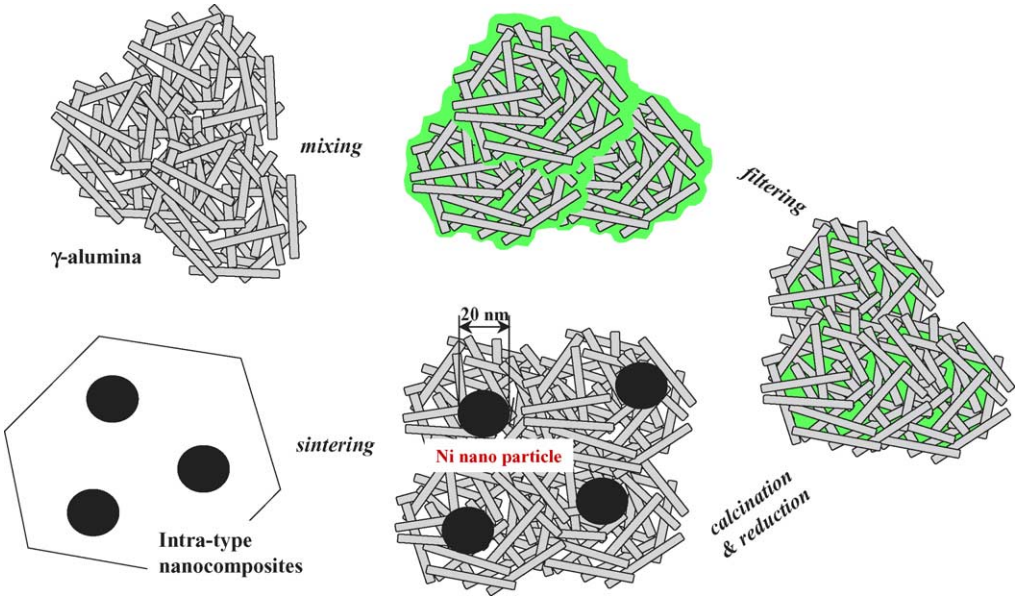

Fig. 7. Schematic explanation of the soaking method.

nano-pores of the γ-alumina. Then, we obtained an intra-type nano-structure of alumina–nickel composites.

3.2. Materials and preparation

Commercially available γ-alumina powder (AKP-G015, Sumitomo Chemical, Japan, 99.99% purity with average agglomerate size 260 nm) was used as a matrix and nickel nitrate (Osaka Chemistry, Japan, 99.9% purity) as a source of nickel particles dispersed in the matrix. To investigate the sinterability of the specimens, we added 10 wt.% of α-alumina (TM-D, Taimei Chemical Co., Japan, average grain size 250 nm) as a seed and 0.25 wt.% MgO as a sintering additive.

Intra-structure of alumina–nickel nanocomposite powders was prepared by the soaking method mentioned above. The mixtures were sintered by the pulse electric current sintering (PECS) method [8] under 30 MPa in vacuum. The samples were sintered at 1350, 1450 and 1550 °C with soaking times of 5 and 60 min. The volume fraction of Ni nanoparticles was about 3 vol.% in these nanocomposites.

3.3. Characterization

Bulk densities of the specimens after sintering were measured by the Archimedes' method. The fracture strength was obtained by a three-point bending test for specimens 2 mm × 2 mm × 20 mm in size and the fracture toughness was measured using a single edged V-notch beam (SEVNB) method [9]. The SEVNB method uses a sharp V-shaped notch to estiamte the intrinsic fracture toughness. After the three-point bending test, the fracture surfaces were observed by SEM.

4. Results and discussion

Fig. 8 shows a micrograph of transmission electron microscopy (TEM) of the γ-alumina powder containing nano-sized nickel grains after reducing at 800 °C in hydrogen atmosphere for 1 h. The pure nickel metallic particles with average grain size of 20 nm were dispersed homogeneously within the γ-alumina agglomerates with column-like primary particles.

Relative densities of the specimens sintered with several temperatures are shown in Fig. 9, where the open marks (○, □, and ◇) indicate the specimens with a soaking time of 5 min, and the solid-circle marks (●) indicate the specimens with a soaking time of 60 min without any addition. The specimens of open-circle marks (○) were sintered without addition, the specimens of open-square marks (□) were sintered with MgO as a sintering additive, and the open-diamond marks (◆) are the specimens sintered with α-alumina as a seed. The figure shows that the specimens with longer soaking time have higher density, especially at lower sintering temperatures and specimens with α-alumina

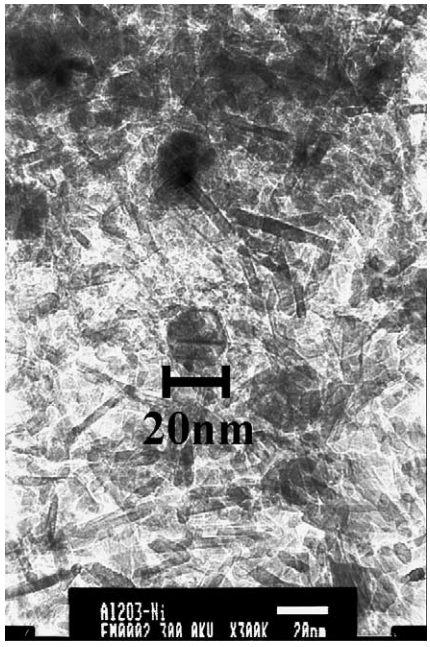

Fig. 8. TEM micrograph for reduced nickel within γ-alumina grains.

seeding and with the sintering additive of MgO markedly improved the relative densities. However, every specimen shows roughly the same density at 1550 °C. From these results, it is noted that the α-alumina seeding is excellent for fabricating dense alumina–nickel nanocomposites.

The fracture strengths measured by the three-point bending test with a specimen size of 2 mm × 2 mm × 10 mm are shown in Fig. 10. The fracture strengths increase with increasing sintering temperature in all specimens except for the seeded specimens sintered at 1550 °C. Specimens soaked for 5 min without seeding, as shown by (○), indicate the lowest values independent of the sintering temperature. The seeded specimens have high strengths; about four times greater than that of the specimens without seeding at 1350 °C. The strength of the specimens soaked for 5 min without seeding sintered at 1550 °C is about 3.5

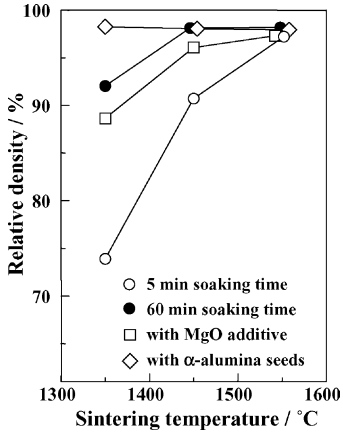

Fig. 9. Relative densities with sintering temperatures of alumina–nickel nanocomposites.

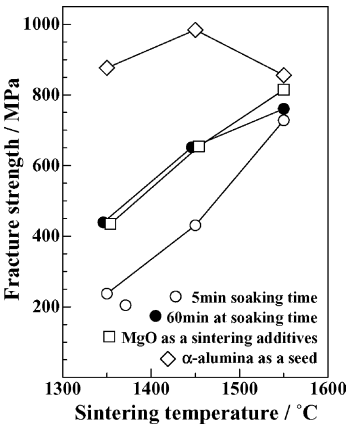

Fig. 10. Fracture strengths with sintering temperatures of alumina–nickel nanocomposites.

times greater than that of the specimen sintered at 1350 °C with no addition.

The fracture surfaces of the specimens were observed by SEM, shown in Fig. 11, where Figs. 11a–c show the micrographs of the specimen without seeding, and Figs. 11d–f show the micrographs of the α-alumina seeded specimens. It is noted that in the non-seeded and seeded specimens, the rate of intra-type fracture mode increased with increasing sintering temperature from 1350 °C (Fig. 11a and d) to 1550 °C (Fig. 11c and f). For the seeded specimens, the strengths increase from 850 MPa of the specimen sintered at 1350 °C to 984 MPa for the specimen sintered at 1450 °C, but the strength decreases at 1550 °C. This can be explained because the melting point of nickel is about 1450 °C, the nickel grains melt and solidify on the grain boundary, then reduce the strength of the nanocomposites. The specimens sintered at 1450 and 1550 °C showed mainly intra-granular fracture mode and several steps are found in the facets on the fracture surface, shown in Fig. 11.

Fig. 12 shows the fracture toughness of the specimens measured using the SEVNB method [7]. The fracture toughness of a specimen without seeding increased with increasing sintering temperature. The highest fracture toughness is obtained in the case of the α-alumina seeded specimens sintered at 1350 °C. But the fracture toughness decreases with increasing the sintering temperature and at 1550 °C every specimen reaches almost the same value ranging from 4.1 to 4.2 MPa $m^{1/2}$. Based on the strengthening and toughening mechanisms of nanocomposites mentioned earlier, it is expected that dislocations generated around the dispersed particles will diffuse outside of the matrix grains at high temperatures. These dislocations reduce the residual stresses in the sintered matrix grains and on the grain boundaries, and these residual stresses will not recover even if the dislocations vanish from the matrix

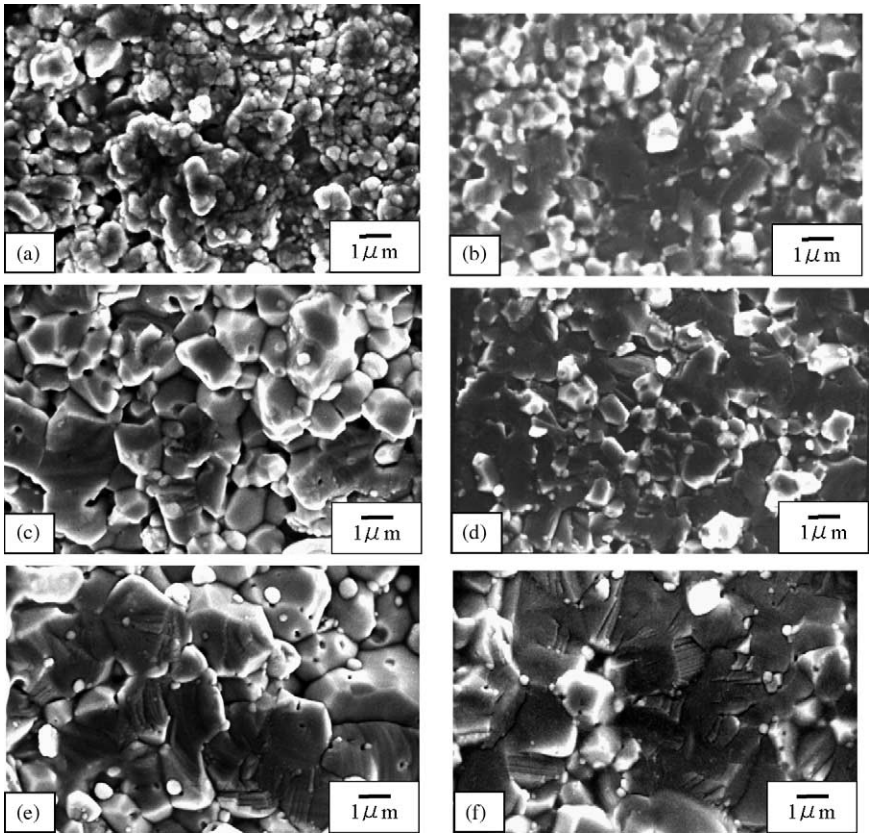

Fig. 11. SEM observations for fracture surfaces on non-seeded specimens shown in the left-side and seeded specimens shown in the right-side, where the sintering temperatures are 1350 °C for (a) and (d), 1450 °C for (b) and (e), and 1550 °C for (c) and (f).

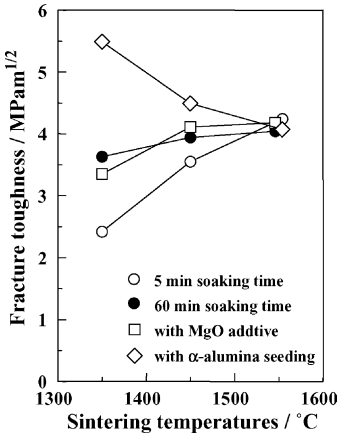

Fig. 12. Fracture toughness vs. sintering temperatures of alumina–nickel nanocomposites.

Table 2
Physical and mechanical properties of γ-Al_2O_3 sintered at 1550 °C by PECS

γ-Alumina as a starting material	
Bulk density (g/cc)	3.9
Relative density (%)	97.8
Vickers' hardness (GPa)	15.8
Young's modulus (GPa)	392.5
Fracture strength (MPa)	601
Fracture toughness (MPa $m^{1/2}$)	4.3

grains. Therefore, the strength of the nanocomposites remains at the improved values due to dispersed particles, even after erasing the dislocations. However, after erasing the dislocations there is no nano-crack nucleus in the matrix. Then the toughening mechanism mentioned above will not work and the fracture toughness of the material reduces to the value of the monolithic matrix with a value around 4.1 MPa $m^{1/2}$, shown in Fig. 12.

Table 2 shows the physical and mechanical properties of γ-alumina sintered at 1550 °C using the PECS technique under the same sintering condition of nanocomposites. Among these properties, the only fracture toughness was measured by the different technique, which was the indentation fracture (IF) method. Almost all the properties, except for the fracture strength, show the same values as those of the nanocomposites sintered at 1550 °C. However, the properties of γ-alumina sintered at lower temperature showed lower values.

5. Conclusions

In this paper, first, strengthening and toughening mechanisms of nanocomposites were summarized on the basis of dislocation activities focusing on the alumina-based nanocomposites. Second, nano-sized nickel dispersed alumina nanocomposites were fabricated using a novel soaking technique to construct intra-type nano-structure, where commercially available γ-alumina powder with high porosity was used as the matrix. Dispersed particles were introduced into the pores using the soaking technique. The alumina powder with nickel oxide particles were then reduced under hydrogen atmosphere and sintered by pulse electric current sintering technique with α-alumina seeding. The maximum strength was 984 MPa for the specimen sintered at 1450 °C and the maximum fracture toughness was 5.5 MPa $m^{1/2}$ for the specimen sintered at 1350 °C.

References

[1] K. Niihara, New design concept of structural ceramics–ceramic nanocomposites, J. Ceram. Soc. Jpn. 99 (1991) 974–981.
[2] R.W. Davidge, R.J. Brook, F. Cambier, M. Poorteman, A. Leriche, D. O'Sullivan, S. Hampshire, T. Kennedy, Fabrication, properties, and modeling of engineering ceramics reinforced with nanoparticles of silicon carbide, Br. Ceram. Trans. 96 (1997) 121–127.
[3] M. Sternitzke, Review: structural ceramic nanocomposites, J. Eur. Ceram. Soc. 17 (1997) 1061–1082.
[4] H. Awaji, S.-M. Choi, E. Yagi, Mechanisms of toughening and strengthening in ceramic-based nanocomposites, Mech. Mater. 34 (2002) 411–422.
[5] S.-M. Choi, S. Honda, T. Nishikawa, H. Awaji, F.D. Gnanam, K. Vishista, T. Kuroyama, Design concept of strengthening and toughening mechanisms in nanocomposites, J. Ceram. Soc. Jpn. 112 (Suppl. 112-1) (2004) S912–S915 (PacRim5 Special Issue).
[6] H. Awaji, S.-M. Choi, Review: Ceramic-Based Nanocomposites, Recent Research Developments in Materials Science and Engineering, vol. 1. Part II, Transworld Research Network, Kerala, 2002, pp. 585–597.
[7] K.P.D. Lagerlöf, A.H. Heuer, J. Castaing, J.P. Rivière, T.E. Mitchell, J. Am. Ceram. Soc. 77 (1994) 385–397.
[8] M. Tokita, Development of automatic FGM manufacturing systems by the spark plasma sintering (SPS) method, functionally graded materials 2000, in: K. Trumble, K. Bowman, I. Reimanis, S. Sampath (Eds.), Ceramic Transactions, vol. 114, 2001, pp. 283–290.
[9] H. Awaji, Y. Sakaida, V-notch technique for single-edge notched beam and chevron notch method, J. Am. Ceram. Soc. 73 (1990) 3522–3523.